



HAL
open science

Tiny changes in tomographic system matrices can cause large changes in reconstruction quality

Feriel Khellaf, Rolf Clackdoyle, Simon Rit, Laurent Desbat

► **To cite this version:**

Feriel Khellaf, Rolf Clackdoyle, Simon Rit, Laurent Desbat. Tiny changes in tomographic system matrices can cause large changes in reconstruction quality. *Physics in Medicine and Biology*, 2022, 67 (10), 10.1088/1361-6560/ac65d5 . hal-03637819

HAL Id: hal-03637819

<https://hal.science/hal-03637819>

Submitted on 11 Apr 2022

HAL is a multi-disciplinary open access archive for the deposit and dissemination of scientific research documents, whether they are published or not. The documents may come from teaching and research institutions in France or abroad, or from public or private research centers.

L'archive ouverte pluridisciplinaire **HAL**, est destinée au dépôt et à la diffusion de documents scientifiques de niveau recherche, publiés ou non, émanant des établissements d'enseignement et de recherche français ou étrangers, des laboratoires publics ou privés.

Tiny changes in tomographic system matrices can cause large changes in reconstruction quality

F. Khellaf¹, R. Clackdoyle¹, S. Rit², L. Desbat¹

¹Univ. Grenoble Alpes, CNRS, Grenoble INP, TIMC-IMAG, 38000 Grenoble, France.

²Université de Lyon, INSA-Lyon, Université Claude Bernard Lyon 1, UJM-Saint Etienne, CNRS, Inserm, CREATIS UMR 5220, U1206, F-69373, Lyon, France.

feriel.khellaf@univ-grenoble-alpes.fr

Abstract

This paper studies the impact of tiny changes in region-of-interest (ROI) tomography system matrices on the variance of the reconstructed ROI. In small-scale and medium-scale examples, the variance in the reconstructed ROI was estimated for different system matrices. The results revealed a striking and counterintuitive phenomenon: a tiny change in the system matrix can dramatically affect the variance of the ROI estimate. In one of our examples, a decrease of 0.1% in one element out of hundreds of thousands of the system matrix resulted in a systematic reduction of the variance inside the ROI, and by a factor of 5 to 10 for some pixels. Our results agree with a recently proven theorem about the ability of additional measurements to reduce the variance in ROI tomography.

1 Introduction

Computed tomography (CT) consists of reconstructing an image from a set of measurements

$$y = Sx + \epsilon \tag{1}$$

with S the $m \times n$ system matrix, x the $n \times 1$ image vector, y the $m \times 1$ measurement vector, and ϵ the $m \times 1$ noise vector. While in classical tomography the whole image x can be reconstructed from the measurements, in region-of-interest (ROI) tomography, only a portion of the image can be uniquely and stably reconstructed (Clackdoyle et al., 2010).

Naturally, as the measured data are noisy, the reconstructed image is not exactly equal to the true image. For both full and ROI tomography, the noise of the solution depends on the input noise vector ϵ , and on the nature of the system matrix S . In this work, we illustrate the impact that tiny variations in the system matrix S can have on the variance of the reconstructed image. Intuitively, we expect that, as long as a pixel can be reconstructed, its variance should vary continuously as a function of the matrix elements. We will show here that this is not always the case in ROI tomography, i.e. there can be a discontinuity in the variance of reconstructible pixels when the elements of the system matrix change slowly.

We note that our work is not a study of the ill-conditioning of tomographic matrices, i.e. the fact that small changes in the data cause a large variance of the reconstructed image. This problem has already been studied, e.g. for under-sampled tomography (Jorgensen et al., 2012). But in the context of ROI tomography, even ill-conditioned matrices can be used to reconstruct unique and stable ROI pixels, and the condition number is not indicative of the stability of the solution in the ROI. In this study, we are interested in how the variance changes with the matrix elements rather than in the value of the variance itself.

We study the variance for full reconstruction and ROI reconstruction using different examples, and show that our results agree with a recently published theorem (Defrise et al., 2021) about the impact of additional measurements on the ROI.

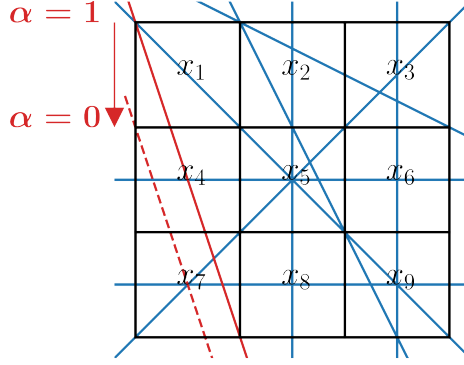


Figure 1: Projection lines used in the full reconstruction system. The projection line corresponding to the last row of S is shown in red.

2 Full reconstruction

We illustrate here the fact that as the system matrix becomes more unstable (approaches a singular matrix), the quality of the reconstruction decreases (the image variance increases). Assuming $\langle \epsilon \rangle = 0$, the discrete model can be rewritten as

$$\langle y \rangle = Sx. \quad (2)$$

We also make the assumption that $\text{cov}(\epsilon) = \sigma^2 I$ with I the $m \times m$ identity matrix. If the matrix S is square and invertible, then the solution is given by

$$\hat{x} = S^{-1}y \quad (3)$$

and

$$\text{cov}(\hat{x}) = \sigma^2 (S^T S)^{-1}. \quad (4)$$

The variance in the reconstructed image \hat{x} is found from the diagonal elements of $\text{cov}(\hat{x})$.

We provide a small-scale example of such a system to illustrate the typical outcome when a system matrix becomes unstable. In all our examples, we use a simple tomographic model of uniform square pixels of unit side length and of constant density, and of ideal line integrals where the contribution of each pixel to the line is equal to the line length through the pixel, scaled by the pixel intensity value. We first considered a 3×3 image and the following 9×9 system matrix

$$S = \begin{pmatrix} 0 & 0 & 0 & 1 & 1 & 1 & 0 & 0 & 0 \\ 0 & 0 & 0 & 0 & 0 & 0 & 1 & 1 & 1 \\ 0 & 1 & 0 & 0 & 1 & 0 & 0 & 1 & 0 \\ 0 & 0 & 1 & 0 & 0 & 1 & 0 & 0 & 1 \\ B & 0 & 0 & 0 & B & 0 & 0 & 0 & B \\ 0 & 0 & B & 0 & B & 0 & B & 0 & 0 \\ 0 & A & 0 & 0 & A & 0 & 0 & 0 & A \\ 0 & A & A & 0 & 0 & 0 & 0 & 0 & 0 \\ \alpha C & 0 & 0 & C & 0 & 0 & C & 0 & 0 \end{pmatrix} \quad (5)$$

where, in the above matrix, the constants A, B, C are $A = \frac{\sqrt{5}}{2}, B = \sqrt{2}, C = \frac{\sqrt{10}}{3}$, and with the parameter α belonging to $(0, 1]$. The measurement lines corresponding to this system matrix are shown in Figure 1. Each value of α corresponds to a different system matrix, where the last measured line has been translated slightly, thus changing a single entry in the matrix. Geometrically, α corresponds to the intersection of this line with the left hand edge of the image, with $1 - \alpha$ being the distance from the upper left corner, measured downwards (see Figure 1).

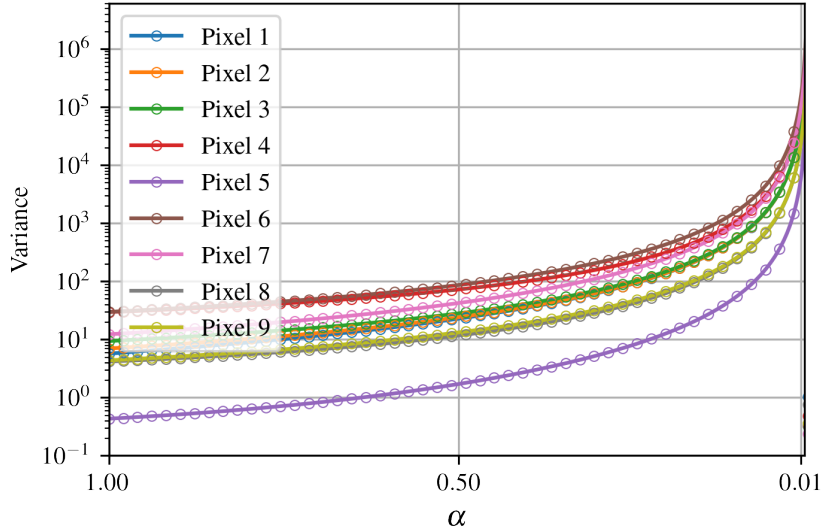


Figure 2: Variance of the 9 pixels, computed analytically (solid line) and numerically (circles), as one matrix entry, $S_{9,1}$, changes linearly from C to zero (i.e. one projection line is translated). Fifty α values between 0 and 1 were used for the numerical tests. Note the logarithmic vertical scale.

When $\alpha = 0$, the last row becomes a linear combination of the others (the linear relationship is $y_9 = y_1 + y_2 - y_3 - y_4 + y_8/A$), and the matrix becomes singular. Otherwise the system is invertible and reconstruction of all pixels is possible. As the matrix becomes singular, we expect that the reconstruction quality will get poorer when there is noise in the measurements. We computed the theoretical variance of reconstruction pixels according to equation (4), and Figure 2 shows that, indeed, the reconstructed variance explodes as the matrix becomes singular.

To confirm these analytical variance calculations, the variance was also estimated numerically from 10^5 reconstructions with Gaussian noise realizations added to the measurements. The 3×3 test image used to compute the numerical variance was a centered 2D Gaussian with a standard deviation of 2 and an amplitude of 5, and we set $\sigma = 1$. The numerical variance calculations are also shown on Figure 2 and they agree with the theoretical behavior: increased noise propagation in the reconstruction as the tomographic system tended towards a singular matrix.

It is usually the case that there are more measurement lines than pixels, in which case $m > n$ and the system is redundant. However, this redundancy opens the (highly likely) possibility for inconsistent data. If $\text{rank}(S) = n$, then a unique least squares solution can be found by using the Moore Penrose generalized inverse:

$$x^\dagger = S^\dagger y \quad (6)$$

with covariance still given by $\sigma^2(S^T S)^{-1}$. (Recall that $S^T S$ is invertible as it is square and has the same rank as S .) Similar reconstructed variance behavior can be observed with overdetermined (redundant) systems as with the simple 9×9 matrix example we showed here. (A 12×9 example can be formed by adding these three rows to the matrix S : $(0, 0, A, 0, 0, A, 0, A, 0)$; $(0, 0, 2D, 0, 0, 2D, 0, D, D)$; $(0, 0, E, 0, 0, 3E/5, 0, 0, 0)$ with $D = \sqrt{29}/10$ and $E = \sqrt{89}/8$. These 3 rows are each linear combinations of the first 8 rows of S , so when $\alpha \rightarrow 0$ the rank again drops to eight. All the pixels then become underdetermined, so the variance behavior of the system is very similar to that of Figure 2).

3 Region-of-interest reconstruction

If $\text{rank}(S) < n$, the system in equation (2) does not have a unique solution, and the Moore-Penrose inverse selects the least squares solution of minimum norm. Region-of-interest reconstruction corresponds to those cases where, while full reconstruction of x is impossible, some

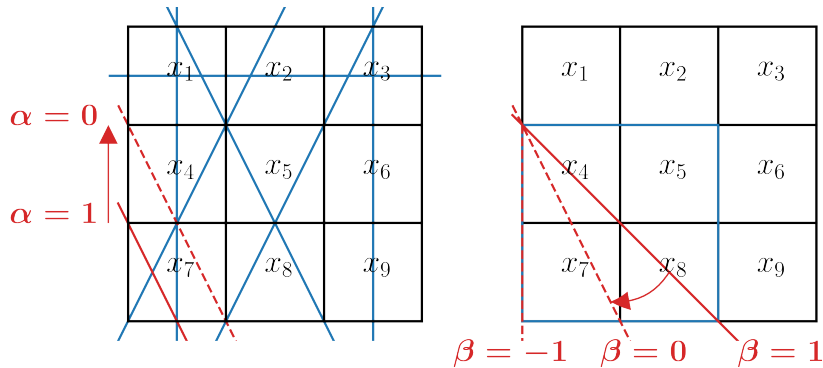


Figure 3: Left: Projection lines used in the ROI reconstruction system of equation (8). Right: The last row of matrix S of equation (9) corresponds to the measurement line that crosses pixel x_4 and exits the bottom of pixel x_7 ($\beta < 0$) or pixel x_8 ($\beta \geq 0$) at a location determined by β .

components of x can be uniquely determined. In this situation of $\text{rank}(S) < n$, the covariance of the Moore-Penrose solution is given by Lewis et al. (1966)

$$\text{cov}(x^\dagger) = \sigma^2(S^T S)^\dagger. \quad (7)$$

We are interested in the reconstructed variance of those pixels. We will illustrate some surprising behavior below, that can occur when the system matrix is changed by one element (or by one measurement line).

3.1 Small-scale examples

We consider the following 7×9 ROI system

$$S = \begin{pmatrix} 1 & 1 & 1 & 0 & 0 & 0 & 0 & 0 & 0 \\ 1 & 0 & 0 & 1 & 0 & 0 & 1 & 0 & 0 \\ 0 & 0 & 1 & 0 & 0 & 1 & 0 & 0 & 1 \\ 0 & A & 0 & A & 0 & 0 & A & 0 & 0 \\ A & 0 & 0 & 0 & A & 0 & 0 & A & 0 \\ 0 & 0 & A & 0 & A & 0 & 0 & A & 0 \\ 0 & 0 & 0 & \bar{\alpha}A & 0 & 0 & A & 0 & 0 \end{pmatrix} \quad (8)$$

where $\bar{\alpha} = 1 - \alpha$, and as before, $A = \sqrt{5}/2$, and $\alpha \in [0, 1]$. The seven corresponding projection lines are shown in Figure 3. This underdetermined system is untypical because pixels x_1 to x_3 can be solved for any value of α (for example: $3x_1 = y_1 + y_2 + (-y_4 + y_5 - y_6)/A$, $3x_2 = y_1 - 2y_2 + (2y_4 + y_5 - y_6)/A$, $3x_3 = y_1 + y_2 + (-y_4 - 2y_5 + y_6)/A$). Our ROI is these three pixels. (It turns out that for certain values of α , the pixels x_4 and x_7 can be reconstructed also.) It can easily be verified that the rank of S is equal to 7 for all α except $\alpha = 0$ when the rank is 6. (Two independent vectors in the nullspace of S are $[0, 0, 0, 0, 0, 1, 0, 0, -1]^T$ and $[0, 0, 0, 0, 1, 0, 0, -1, 0]^T$, and additionally when $\alpha = 0$, $[0, 0, 0, 1, 0, 0, -1, 0, 0]^T$.)

Using equation (7), we computed the variance analytically for the 3 ROI pixels, and we have plotted the variance (solid lines in Figure 4). Note that for both the full system matrices of equation (5) and the ROI matrices of equation (8), the rank of the matrix decreases by one when α reaches zero. However, as $\alpha \rightarrow 0$, the variance increases dramatically in the full system case, whereas the variance remains constant for the ROI case. Even more surprising, the variance jumps to a lower value in the ROI case when α reaches zero. So the ROI can be reconstructed *better* when the rank of the system matrix drops, and in this case, with just a tiny change in one entry of the matrix. We verified the variance numerically in the ROI pixels, using the same test image. Figure 4 shows the agreement of the numerical simulations with the theoretically calculated variance of the three ROI pixels.

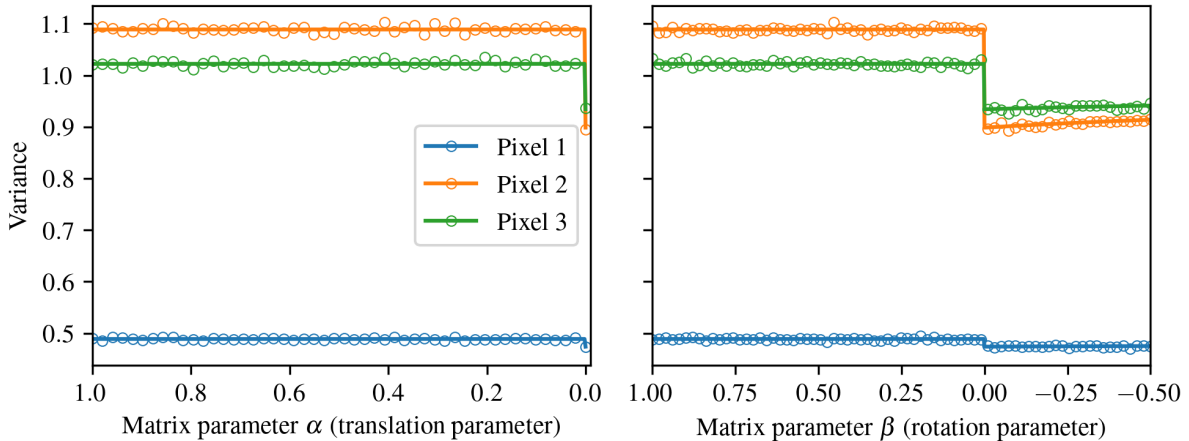


Figure 4: Variance of the 3 ROI pixels, computed analytically (solid line) and numerically (circles), as the projection line is translated (left) or rotated (right).

We examined a second similar small scale example, using a matrix identical to that of equation (8) except for the seventh (the last) row, which is parameterized by $\beta \in [-1, 1]$:

$$S = \begin{pmatrix} 1 & 1 & 1 & 0 & 0 & 0 & 0 & 0 & 0 \\ 1 & 0 & 0 & 1 & 0 & 0 & 1 & 0 & 0 \\ 0 & 0 & 1 & 0 & 0 & 1 & 0 & 0 & 1 \\ 0 & A & 0 & A & 0 & 0 & A & 0 & 0 \\ A & 0 & 0 & 0 & A & 0 & 0 & A & 0 \\ 0 & 0 & A & 0 & A & 0 & 0 & A & 0 \\ 0 & 0 & 0 & F_4 & 0 & 0 & F_7 & F_8 & 0 \end{pmatrix} \quad (9)$$

where, as before, $A = \sqrt{5}/2$, and where

$$F_4 = \frac{\sqrt{\beta^2 + 2\beta + 5}}{2} \quad (10)$$

$$F_7 = \begin{cases} \left(1 - \frac{2\beta}{1+\beta}\right)F_4 & \beta \in (0, 1] \\ F_4 & \beta \in [-1, 0] \end{cases} \quad (11)$$

$$F_8 = \begin{cases} \frac{2\beta}{1+\beta}F_4 & \beta \in (0, 1] \\ 0 & \beta \in [-1, 0] \end{cases} \quad (12)$$

Here we have the same ROI of $\{x_1, x_2, x_3\}$, and it turns out that no other pixels can be resolved for this system, irrespective of the value of β . (A direct calculation reveals that only the x_1, x_2 , and x_3 axes, and no others, are perpendicular to the nullspace of S .) Note that when $\alpha = 0$ and $\beta = 0$, the two matrices (of equations (8) and (9)) are identical. The measurement line corresponding to the last row is described as follows. The parameter β lies on the bottom horizontal line of the image pixels, with $\beta = 0$ corresponding to the line separating (unit) pixels x_7 and x_8 as shown in Figure 3. The measurement line corresponding to a value of $\beta \in [-1, 1]$ starts in the upper left corner of pixel x_4 and meets the lower boundary of the image at the value β . At most three matrix entries are involved for any value of β : entries $S_{7,4}, S_{7,7}, S_{7,8}$. The three corresponding line-lengths for these pixels are given by equations (10), (11) and (12).

The analytically computed and numerically estimated variances in the ROI pixels are shown in Figure 4 for $\beta \in [-1/2, 1]$. The analytic calculations showed that for $\beta > 0$, the reconstructed variance in the 3 ROI pixels remained the same, even though three of the matrix values were

approaching the critical $\beta = 0$ where the rank of the matrix changed. At that point the variances abruptly decreased, and remained fairly constant (with a slight upward slope in Figure 4) as β became more negative. Two new features in this example are (i) there is no change in the number of pixels that can be reconstructed when the matrix passes the critical point ($\beta = 0$), and (ii) the change in variance is sustained, not an apparently instantaneous "blip".

To verify that there is a discontinuity in the reconstructed variances even for extremely small changes in the last measurement line, the variance modifications corresponding to changes in α of 0.001 (for the first ROI matrix) and changes in β of 0.0005 (for the second ROI matrix) are given in Table 1. For pixel 2, for example, the variance jumped by more than 20% following a tiny change in the measurement line, confirming that the variance in the ROI is not continuous as a function of the system matrix elements.

Table 1: Theoretical variances in the ROI pixels when a small variation is applied to one measurement line.

	$\alpha = \beta = 0$	$\alpha = 0.001$	$\beta = 0.0005$
Pixel 1	0.474	0.489	0.489
Pixel 2	0.899	1.089	1.089
Pixel 3	0.934	1.022	1.022

3.2 A medium-scale example

The small-scale problems present simple and easily reproducible examples. We also considered a larger 32×32 pixel image of the Shepp-Logan phantom (Shepp et al., 1974) with a 16×16 square ROI in the upper left corner. A 392×1024 system matrix was built to reconstruct the ROI. Amongst those 392 measurements, 288 were necessary to uniquely reconstruct the ROI pixels (we built an intermediate full rank system comprised of the 16×16 ROI pixels plus 2×16 grouped pixels corresponding to the horizontal pixel lines of the upper right corner and the vertical pixel lines of the lower left corner). Other measurements were added to include all 32×32 pixels in the system, "break" grouped pixels (identical columns in the system matrix) and add some redundancy. The reference Shepp-Logan phantom and the corresponding pseudo-inverse reconstruction from the 392 noise-free measurements are shown in Figure 5.

Similar to the first ROI example of equation (8), we allowed one element of the system matrix to vary: $S_{392,513} = (\sqrt{257}/16)\bar{\alpha}$. Note from figure 5 that pixel 513 and measurement line 392 are peripheral and do not involve the 16×16 ROI region. Geometrically, increasing α from 0 corresponds to translating the last measurement line downwards, just as in the first ROI example. For non-zero α , the matrix had rank 368, and for $\alpha = 0$, the rank was 367. We examined the reconstructed variance for the two system matrices corresponding to $\alpha = 0$ and $\alpha = 0.001$. These two matrices differed in only one of the 401,408 matrix elements, and by a tiny amount: 1.00195 became 1.00095. We evaluated the impact of this small variation on the ROI analytically and numerically. The variance of the noise was again set to $\sigma^2 = 1$.

The results are shown in Figure 6. The variance of the pixels reconstructed using $\alpha = 0$ was smaller than when using $\alpha = 0.001$. With $\alpha = 0$, the reconstructed variance was reduced in nearly every ROI pixel, about 10% on average and up to 89%. The numerical variances are shown, but the theoretical and experimental calculations agreed well (the largest differences were less than 2%).

4 Discussion

Our observations have shown that, in the case of ROI reconstruction, the variance of reconstructible pixels does not always depend continuously on the matrix entries. We saw that a minuscule change of just one matrix entry can result in jumps in the reconstructed variances of all the ROI pixels.

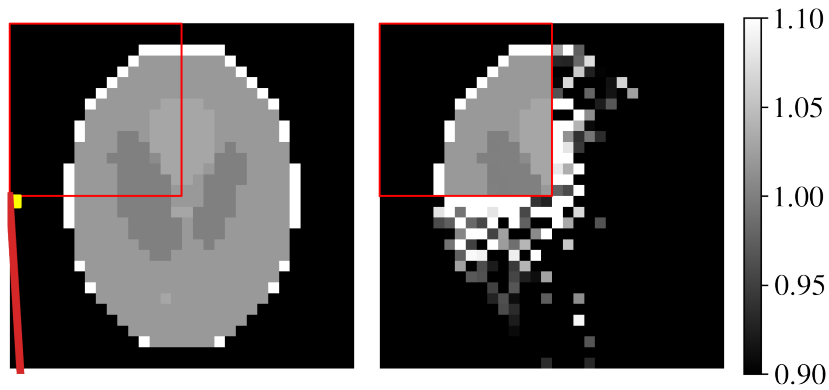


Figure 5: Reference Shepp-Logan phantom (left) and reconstruction from noise-free data (right), with the ROI pixels indicated by the red square. The 392nd measurement line is shown in red and pixel 513 in yellow.

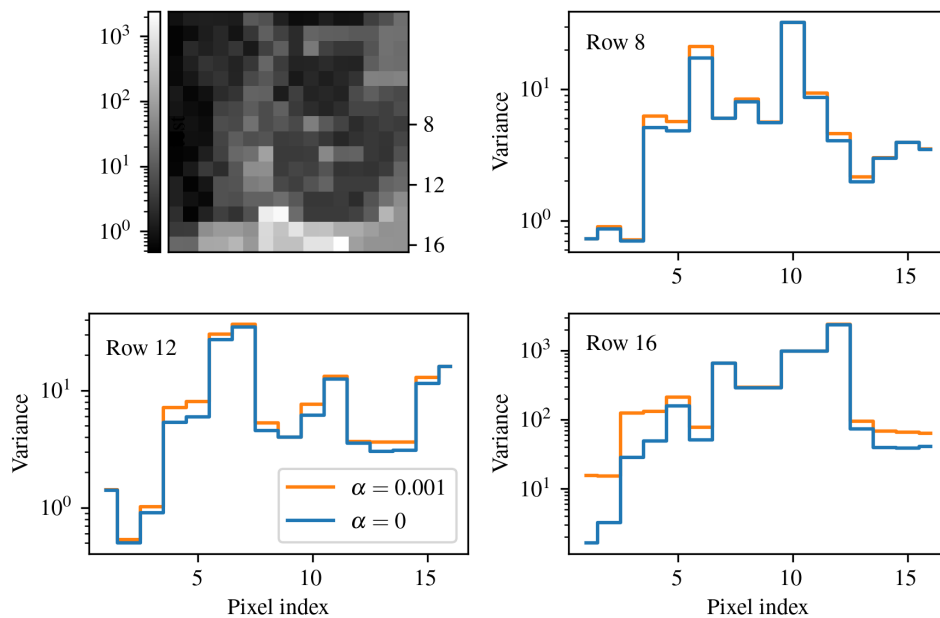


Figure 6: Top left: variances of the 16×16 pixels in the ROI reconstructed with $\alpha = 0.001$. Top right, bottom left and right: horizontal profiles through the variance images reconstructed using either $\alpha = 0$ or $\alpha = 0.001$. The shown variances were computed numerically. Note the logarithmic scale.

Close examination of the small-scale examples can provide some explanations for this remarkable behavior. Both matrices (equations (8) and (9)) had the same first six rows, and the pixel values x_1, x_2, x_3 could be found from the first six measurement values y_1, y_2, \dots, y_6 . Now, for α and β both nonzero, the two matrices are both full rank (with rank 7) so in both cases the last row is not a combination of the other six rows. On the other hand, when $\alpha = \beta = 0$ the two matrices are the same, and the rank drops to 6, because the seventh row is now a linear combination of the first six rows. This new redundancy provided by the seventh row allows y_7 to contribute to the solution for x_1, x_2, x_3 , thereby improving the accuracy of the solution in the presence of noise.

The ROI pixels x_1, x_2, x_3 can be solved using the first six rows of the matrix, and for the full rank situation of α and β both non-zero, the seventh row is not helpful. This statement is a consequence of a theorem published recently (Defrise et al., 2021). The essence of that theorem is that if the new row (or rows) of the matrix are independent of the existing rows, then there will be no improvement in the reconstructed variance of the ROI pixels.

5 Conclusion

We have shown a remarkable and seemingly counterintuitive phenomenon: a tiny alteration of the system matrix of a ROI problem can drastically change the variance of the reconstructed pixel values in the ROI. We note that this effect occurs when the system matrix changes rank, and, surprisingly, improved reconstruction occurred with lower rank of the matrix. We linked this result to a recently published theorem on ROI reconstruction.

Acknowledgements

This work was partially supported by grant ANR-17-CE19-0006 (ROI doré project) from the Agence Nationale de la Recherche.

References

- Clackdoyle, R. and M. Defrise (2010). “Tomographic reconstruction in the 21st century”. In: *IEEE Signal Processing Magazine* 27.4, pp. 60–80.
- Defrise, M., R. Clackdoyle, L. Desbat, F. Noo, and J. Nuyts (2021). “Do additional data improve region-of-interest reconstruction?” In: *Proceedings of the 16th Virtual International Meeting on Fully 3D Image Reconstruction in Radiology and Nuclear Medicine*. (Leuven, Belgium). Ed. by Y. Berbers and W. Zwaenepoel, pp. 38–43.
- Jorgensen, J. S., E. Y. Sidky, and X. Pan (2012). “Quantifying admissible undersampling for sparsity-exploiting iterative image reconstruction in X-ray CT”. In: *IEEE Transactions on Medical Imaging* 32.2, pp. 460–473.
- Lewis, T. and P. Odell (1966). “A generalization of the Gauss-Markov theorem”. In: *Journal of the American Statistical Association* 61.316, pp. 1063–1066.
- Shepp, L. A. and B. F. Logan (1974). “The Fourier reconstruction of a head section”. In: *IEEE Transactions on nuclear science* 21.3, pp. 21–43.